

Distinct mechanisms for OxLDL uptake and cellular trafficking by class B scavenger receptors CD36 and SR-BI

Bing Sun,^{1,*} Boris B. Boyanovsky,^{1,†} Margery A. Connelly,[§] Preetha Shridas,[†]
Deneys R. van der Westhuyzen,^{*,†,**} and Nancy R. Webb^{2,*}

Graduate Center for Nutritional Sciences,^{*} Department of Internal Medicine,[†] and Department of Molecular and Cellular Biochemistry,^{**} University of Kentucky Medical Center, Lexington, KY 40536; and Johnson & Johnson Pharmaceutical Research and Development, LLC,[§] Spring House, PA 19477-0776

Abstract Modified forms of LDL, including oxidized low density lipoprotein (OxLDL), contribute to macrophage lipid accumulation in the vessel wall. Despite the pathophysiological importance of uptake pathways for OxLDL, the molecular details of OxLDL endocytosis by macrophages are not well understood. Studies in vitro demonstrate that the class B scavenger receptor CD36 mediates macrophage uptake and degradation of OxLDL. Although the closely related scavenger receptor class B type I (SR-BI) binds OxLDL with high affinity, evidence that SR-BI plays a role in OxLDL metabolism is lacking. In this study, we directly compared OxLDL uptake and degradation by CD36 and SR-BI. Our results indicate that although CD36 and SR-BI internalize OxLDL, SR-BI mediates significantly less OxLDL degradation. Endocytosis of OxLDL by both SR-BI and CD36 is independent of caveolae, microtubules, and actin cytoskeleton. However, OxLDL uptake by CD36, but not SR-BI, is dependent on dynamin. The analysis of chimeric SR-BI/CD36 receptors shows that the CD36 C-terminal cytoplasmic tail is necessary and sufficient for dynamin-dependent OxLDL internalization by class B scavenger receptors. These findings indicate that different mechanisms are involved in OxLDL uptake by SR-BI and CD36, which may segregate these two structurally homologous receptors at the cell surface, leading to differences in intracellular trafficking and degradation.—Sun, B., B. B. Boyanovsky, M. A. Connelly, P. Shridas, D. R. van der Westhuyzen, and N. R. Webb. **Distinct mechanisms for OxLDL uptake and cellular trafficking by class B scavenger receptors CD36 and SR-BI.** *J. Lipid Res.* 2007. 48: 2560–2570.

Supplementary key words atherosclerosis • endocytosis • dynamin • scavenger receptor class B type I • oxidized low density lipoprotein

Macrophage binding and uptake of oxidized low density lipoprotein (OxLDL) has been proposed to play a key role

in the initiation of atherosclerotic lesion development, the formation of lipid-laden foam cells. CD36 is one of several OxLDL receptors contributing to this process (1, 2). CD36 is an 88 kDa plasma membrane glycoprotein that binds a diverse array of ligands in addition to OxLDL, including thrombospondin-1 (3), the native lipoproteins LDL, HDL, and VLDL (4), long-chain fatty acids (5), anionic phospholipids (6), and apoptotic cells (7). As a result of its broad specificity, CD36 has been reported to contribute to various normal and pathologic processes, such as apoptotic cell clearance, fatty acid transport, angiogenesis, atherosclerosis, inflammation, and lipid metabolism (reviewed in Ref. 8). CD36 is expressed in a range of cells and tissues that includes monocytes/macrophages, platelets, mammary epithelial cells, vascular endothelial cells, and adipose tissues (9). Studies performed ex vivo indicate that 60–70% of macrophage foam cell formation induced by OxLDL may be CD36-dependent (10–12). CD36-mediated OxLDL degradation has been reported in cell lines in addition to macrophages, including adipocytes (13). Studies in Chinese hamster ovary (CHO) cells transfected with CD36 cDNA and C32 cells with endogenous expression of CD36 have investigated CD36 trafficking after OxLDL binding. The results indicate that binding of OxLDL to CD36 leads to the internalization of CD36 and OxLDL into endosomal compartments that do not contain caveolin-1 or transferrin but do contain a glycosylphosphatidylinositol-anchored lipid raft protein decay-accelerating factor (14). Thus, CD36 appears to endocytose OxLDL through a nonclathrin, noncaveolar, lipid raft-mediated pathway. Studies using site-directed mutagenesis demonstrate that the C-terminal six amino

Abbreviations: CHO, Chinese hamster ovary; MFI, mean fluorescence intensity; OxLDL, oxidized low density lipoprotein; SR-BI, scavenger receptor class B type I; VSMC, vascular smooth muscle cell.

¹ B. Sun and B. B. Boyanovsky contributed equally to this work.

² To whom correspondence should be addressed.

e-mail: nrwebb1@uky.edu

Manuscript received 2 April 2007 and in revised form 27 August 2007 and in re-revised form 17 September 2007.

Published, JLR Papers in Press, September 19, 2007.
DOI 10.1194/jlr.M700163-JLR200

acids of the CD36 cytoplasmic tail are critical for the binding and endocytosis of OxLDL (15).

Scavenger receptor class B type I (SR-BI) is another class B scavenger receptor closely related to CD36 (16). The membrane topology of SR-BI is similar to that of CD36, such that both receptors contain a large extracellular domain flanked by short N- and C-terminal cytoplasmic domains. The two receptors share sequence similarity (35%) throughout their entire extracellular domains. SR-BI is best known as a physiological HDL receptor, but it can bind a broad range of other lipoprotein ligands, including LDL, OxLDL, and acetylated LDL (16, 17). Indeed, OxLDL binding to SR-BI reportedly occurs at relatively higher affinity (dissociation constant $\sim 4 \mu\text{g/ml}$) compared with HDL binding to SR-BI (dissociation constant $\sim 50 \mu\text{g/ml}$) (18). Consistent with its role as an HDL receptor, SR-BI is most highly expressed in liver and steroidogenic tissues. However, SR-BI is also present in monocytes/macrophages and human and mouse atherosclerotic lesions (19–21). SR-BI expressed in transfected CHO cells mediates the uptake and degradation of OxLDL (18), but the molecular mechanism and *in vivo* significance of this uptake have not been defined.

Although CD36 and SR-BI have been shown to bind OxLDL with similar high affinity, the metabolism of OxLDL by these two class B scavenger receptors has not been compared directly. In this study, we determined that CD36 and SR-BI differ in their ability to internalize and degrade OxLDL. Experiments to define the fate and intracellular trafficking of OxLDL after SR-BI or CD36 binding indicate that distinct mechanisms are involved in OxLDL uptake by these two receptors, which appear to lead to differences in intracellular trafficking and the extent of lysosomal degradation.

EXPERIMENTAL PROCEDURES

Cells

COS-7 cells were originally obtained from the American Type Culture Collection (Manassas, VA) and maintained in DMEM supplemented with 2 mM L-glutamine, 50 U/l penicillin G, 50 $\mu\text{g/l}$ streptomycin, and 10% heat-inactivated fetal calf serum (all from Invitrogen, Carlsbad, CA). Peritoneal macrophages were obtained from C57BL/6 mice (Jackson Laboratory, Bar Harbor, ME) and CD36-deficient mice (provided by R. L. Silverstein) (22) using procedures that were reviewed and approved by the Lexington Veterans Affairs Institutional Animal Care and Use Committee. Animals were injected intraperitoneally with a sterile solution (1 ml) of 1% Biogel 100 (Bio-Rad) in phosphate-buffered saline. After 96 h, the animals were anesthetized, and peritoneal macrophages were harvested by lavage with 5 ml of ice-cold phosphate-buffered saline. Macrophages were seeded on glass coverslips in 12-well dishes at a density of $\sim 2.0 \times 10^6$ cells/well in DMEM supplemented with 10% fetal bovine serum, 100 U/ml penicillin/streptomycin, 2 mM L-glutamine, and 25 ng/ml macrophage colony-stimulating factor (Calbiochem) and allowed to attach for 4 h. Nonattached cells were then removed by washing the dishes with phosphate-buffered saline. Macrophages were incubated in supplemented DMEM overnight at 37°C before the experiments.

Expression of CD36, SR-BI, CD36/SR-BI chimeras, and dynK44A in COS-7 cells

COS-7 cells were transiently transfected with murine SR-BI or CD36 using the Lipofectamine™ transfection reagent as directed by the manufacturer (Invitrogen). The next day, cells were replated in 12-well cluster dishes and incubated for an additional 24 h before uptake assays. For studies of chimeric CD36/SR-BI receptors, COS cells were cotransfected with pSV2neo along with expression plasmids encoding wild-type rat CD36, mouse SR-BI, CD/SRT, or SR/CDT (23, 24). Stable transfectants were propagated in medium containing 0.5 mg/ml G418. Alternatively, SR-BI or CD36 was expressed in COS-7 cells using the adenoviral vectors AdSR-BI and AdCD36 using a multiplicity of infection of 5,000 particles/cell (25, 26). In some experiments, dynK44A (a dominant negative mutant of dynamin 1 that inhibits dynamin function) was coexpressed by adenoviral vector (generously provided by Dr. D. L. Silver) (27). Cells were seeded in 10 cm dishes, and when $\sim 80\%$ confluent, inoculated with adenoviral vectors. Twenty-four hours after inoculation, cells were reseeded in 12-well clusters and incubated at 37°C for an additional 24 h before the addition of ligands. To confirm SR-BI and CD36 expression, Western blot analysis of representative cell lysates was performed as described previously (25, 26).

Preparation of OxLDL, Alexa488-OxLDL, ^{125}I -OxLDL, and ^{125}I -transferrin

The LDL ($d = 1.019\text{--}1.063 \text{ g/ml}$) fraction was isolated from fresh human plasma by density gradient ultracentrifugation as described previously (28). Isolated fractions were dialyzed against 150 mM NaCl and 0.01% EDTA, sterile-filtered, and stored under argon gas at 4°C. Protein concentrations were determined by the method of Lowry et al. (29). Native LDL (2 mg/ml) was dialyzed against 150 mM NaCl to remove EDTA and then dialyzed against 5 μM CuSO₄ overnight at 4°C, followed by 6 h at room temperature with minimal stirring. Oxidation was terminated with 10 mM EDTA and dialysis against 150 mM NaCl and 0.01% EDTA to remove CuSO₄. The relative mobility of OxLDL compared with native LDL electrophoresed on a 1.8% agarose gel for 1 h at 100 V was ~ 1.8 . Thus, the relative mobility of our OxLDL preparations corresponds to the “mildly” OxLDL described by Kunjathoor et al. (10) (relative mobility ~ 2.0), which has been shown to be preferentially internalized by macrophages via CD36. OxLDL apolipoproteins and mouse transferrin (Sigma, St. Louis, MO) were iodinated in the presence of ^{125}I (Amersham Biosciences, Piscataway, NJ) by the iodine monochloride method (30). Alternatively, OxLDL was covalently modified with Alexa488 (Molecular Probes, Eugene, OR) according to the manufacturer's directions. Labeled OxLDL preparations were stored under argon gas at 4°C and used for experiments within 3 weeks.

Association and degradation assays

Control COS-7 cells and COS-7 cells expressing CD36 (COS-CD36) or SR-BI (COS-SRBI) with or without coexpression of dynK44A were incubated at 37°C with 10 $\mu\text{g/ml}$ ^{125}I -OxLDL for 4 h. As a control, cells were similarly incubated with 25 $\mu\text{g/ml}$ ^{125}I -labeled transferrin for 15 min at 37°C. After the incubation, the medium was collected and cells were washed three times with ice-cold washing buffer (50 mM Tris, 150 mM NaCl, and 2 mg/ml fatty acid free BSA) followed by two washes with washing buffer without BSA to remove unbound ligand. All washes were performed at 4°C with prechilled solutions. The cells were then solubilized in 0.1 N NaOH for 60 min at room temperature, and cellular protein and radioactivity content were measured. ^{125}I present in the lysate corresponded to cell-associated OxLDL

protein or transferrin. The trichloroacetic acid-soluble degraded material in cell medium was assayed as described previously (31). In all experiments, receptor-specific values were calculated as the difference between values from receptor-expressing COS-7 cells and control cells. The amount of cell-associated and degraded ^{125}I for control cells did not exceed 10% of the corresponding values for receptor-expressing cells.

Fluorescence energy transfer assay for measurement of intracellular OxLDL

Intracellular accumulation of OxLDL was quantified using a fluorescence-based assay described previously by our laboratory (32). COS-7, COS-CD36, and COS-SRBI cells with and without dynK44A expression were incubated at 37°C with 10 $\mu\text{g}/\text{ml}$ Alexa488-OxLDL and then collected from the dish by gentle rinsing. The cells were subsequently incubated with or without trypan blue (0.4% solution in PBS; Cellgro, Richmond, VA) at 4°C for 15 min and washed once in PBS before analysis. To quantify intracellular accumulation of Alexa488-OxLDL, cells were analyzed by flow cytometry, and cell-surface OxLDL was estimated by calculating the difference in mean fluorescence intensity (MFI) in cells with or without trypan blue. The percentage of total cell-associated OxLDL that was intracellular was calculated by dividing the MFI of cells in the presence of trypan blue by the MFI of cells in the absence of trypan blue. In all experiments, CD36- or SR-BI-specific MFIs were calculated as the difference between values from COS-CD36 and COS-SRBI cells and control COS-7 cells. For time course studies, Alexa488-OxLDL was added to the cells at staggered intervals so that cells were harvested at the same time. For experiments using inhibitors, cells were preincubated at 37°C with or without 25 $\mu\text{g}/\text{ml}$ nystatin (N6261; Sigma), 10 μM nocodazole (M1404; Sigma), or 10 μM cytochalasin D (C8273; Sigma) for 1 h. Cells were then incubated with 10 $\mu\text{g}/\text{ml}$ Alexa488-OxLDL at 37°C for 1 h in the presence of the same drug concentrations.

Fluorescence microscopy

For analysis by confocal microscopy, COS-7, COS-CD36 and COS-SRBI cells were seeded on glass coverslips in 12-well cluster dishes and incubated at 37°C for an additional 24 h. For pulse-chase experiments, cells were incubated with 20 $\mu\text{g}/\text{ml}$ Alexa488-OxLDL at 37°C for 30 min, washed three times with PBS to remove unbound material, and then processed immediately (0 min chase) or incubated with fresh medium without fluorescent ligand for an additional 30 or 90 min. In all cases, Alexa568-transferrin (Invitrogen) was added during the last 15 min of incubation. Cells were fixed with 4% formaldehyde (pH 7.2) at room temperature for 15 min and then washed two times with PBS. Coverslips were mounted on slides using fluorescence-protecting medium (Vectashield; Vector Laboratories, Burlingame, CA) and analyzed with an Olympus BX51 fluorescence microscope or a Leica TCS confocal laser scanning fluorescence microscope using a 60 \times oil-immersion objective and argon (488 nm) and krypton (568 nm) lasers. For experiments using inhibitors, cells were preincubated with 25 $\mu\text{g}/\text{ml}$ nystatin, 10 μM nocodazole, or 10 μM cytochalasin D at 37°C for 1 h. Cells were then incubated with 10 $\mu\text{g}/\text{ml}$ Alexa488-OxLDL in the presence of the same drug concentration at 37°C for 1 h.

The efficacy of dynK44A or nystatin inhibition was assessed in control experiments, whereby COS-7 cells were incubated with Alexa488-transferrin (15 min) or Alexa488-albumin (Molecular Probes) (30 min), respectively. To assess the effect of cytochalasin D treatments, cells were fixed with 4% formaldehyde and then incubated with rhodamine phalloidin (R415; Molecular Probes) at room temperature for 1 h. In another control exper-

iment, COS-7 cells with or without preincubation with 10 μM nocodazole at 37°C for 1 h were fixed with 4% formaldehyde and then permeabilized with 0.1% Triton X-100. Cells were washed and incubated with FITC-conjugated monoclonal primary antibody against tubulin (1:200, Sigma) at room temperature for 1 h. For OxLDL-dynamin colocalization experiments, mouse peritoneal macrophages were incubated with Alexa568-OxLDL for 1 h, fixed in 10% formalin for 15 min, washed two times with PBS, and blocked for 1 h at room temperature with PBS containing 5% normal goat serum and 0.5% Triton X-100. Cells were then incubated for 1 h at room temperature with a mouse monoclonal anti-dynamin antibody (Abcam, Cambridge, MA). After four washes with 0.2% Tween in PBS, dynamin was detected using Alexa488-labeled goat anti-mouse IgG (1:200; Molecular Probes).

Data and statistical analysis

Data are expressed as means \pm SEM. Results were analyzed by Student's *t*-test. Differences were considered statistically significant at $P < 0.05$.

RESULTS

CD36 mediates more efficient OxLDL degradation than SR-BI

To compare OxLDL degradation by the two class B scavenger receptors, CD36 or SR-BI was expressed in COS-7 cells and receptor-specific OxLDL degradation was determined. Cell association and degradation of ^{125}I -OxLDL for control COS-7 cells did not exceed 10% of the corresponding values for receptor-expressing cells (data not shown). After 4 h of incubation with ^{125}I -OxLDL at 37°C, COS-CD36 cells mediated \sim 2-fold more OxLDL degradation compared with COS-SRBI cells (Fig. 1A), normalized for cell-associated OxLDL. This result indicates that although both CD36 and SR-BI are OxLDL receptors, CD36 mediates more efficient OxLDL degradation than SR-BI.

CD36 and SR-BI mediate intracellular accumulation of OxLDL

We investigated whether the difference in OxLDL degradation by CD36 and SR-BI could be attributed to differences in the extent to which the two receptors mediate OxLDL internalization. Uptake of OxLDL by COS-CD36 and COS-SRBI cells was quantified in five separate experiments using different batches of transiently transfected cells by our previously described fluorescence energy transfer assay, in which the fluorescence of cell surface Alexa488-OxLDL, but not intracellular Alexa488-OxLDL, is specifically quenched by trypan blue (32). COS-CD36 and COS-SRBI cells were incubated with Alexa488-OxLDL, and the intracellular and cell surface accumulation of OxLDL was determined using flow cytometry (Fig. 1B). When measured at 1 h, $54.4 \pm 5.0\%$ of total cell-associated OxLDL was intracellular in COS-CD36 cells. This compares with COS-SRBI cells, in which $40.3 \pm 4.3\%$ was intracellular. Although the difference in intracellular accumulation was not significant for the two cell types ($P = 0.08$), our data suggest that OxLDL may be taken up

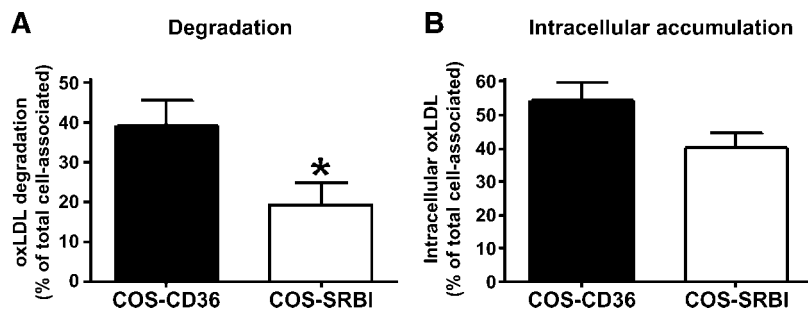


Fig. 1. Oxidized low density lipoprotein (OxLDL) degradation and internalization mediated by scavenger receptor class B type I (SR-BI) and CD36. **A:** COS-7 cells expressing SR-BI or CD36 were incubated with 10 $\mu\text{g}/\text{ml}$ ^{125}I -OxLDL. After 4 h of incubation at 37°C, OxLDL apolipoprotein cell association and degradation were measured. Results are expressed as the percentage of cell-associated OxLDL that was degraded in 4 h. CD36- and SR-BI-specific values are shown, which are defined as the difference in cell-associated radioactivity between CD36/SR-BI-expressing cells and nontransfected COS-7 cells. Values are means \pm SEM of three independent experiments, each done in triplicate. * $P < 0.05$. **B:** COS-7 cells expressing CD36 or SR-BI were incubated with 10 $\mu\text{g}/\text{ml}$ Alexa488-OxLDL at 37°C for 1 h. Cells were washed, incubated with or without 0.4% trypan blue at 4°C for 15 min to quench surface-bound fluorescence, and then subjected to flow cytometry. Intracellular OxLDL, expressed as the percentage of total cell-associated OxLDL, was calculated as the ratio of the mean fluorescence intensity (MFI) in the presence and absence of trypan blue. CD36- and SR-BI-specific values are shown and are means \pm SEM of five independent experiments.

by the two receptors at different rates. Additional studies to quantify intracellular OxLDL after 15, 30, 120, and 240 min incubations consistently showed greater, albeit nonsignificant, OxLDL accumulation in COS-CD36 cells compared with COS-SRBI cells (data not shown).

OxLDL taken up by CD36- and SR-BI-expressing cells traffics through a transferrin-positive intracellular compartment

As another approach to assess OxLDL uptake by the two class B scavenger receptors, we performed a pulse-chase

study in which COS-CD36 and COS-SRBI cells were incubated with Alexa488-OxLDL (green fluorescence) for 30 min, washed to remove unbound ligand, and then analyzed by confocal microscopy after a 0, 30, or 90 min chase interval (**Fig. 2**). Alexa568-transferrin (red fluorescence) was used as a marker for the endocytic recycling compartment. In the case of COS-CD36 cells, OxLDL was easily visualized inside the cells after the 30 min incubation (0 min chase), which accumulated in a discrete perinuclear region, apparently colocalized with transferrin (indicated by arrows). In contrast, colocalization of OxLDL

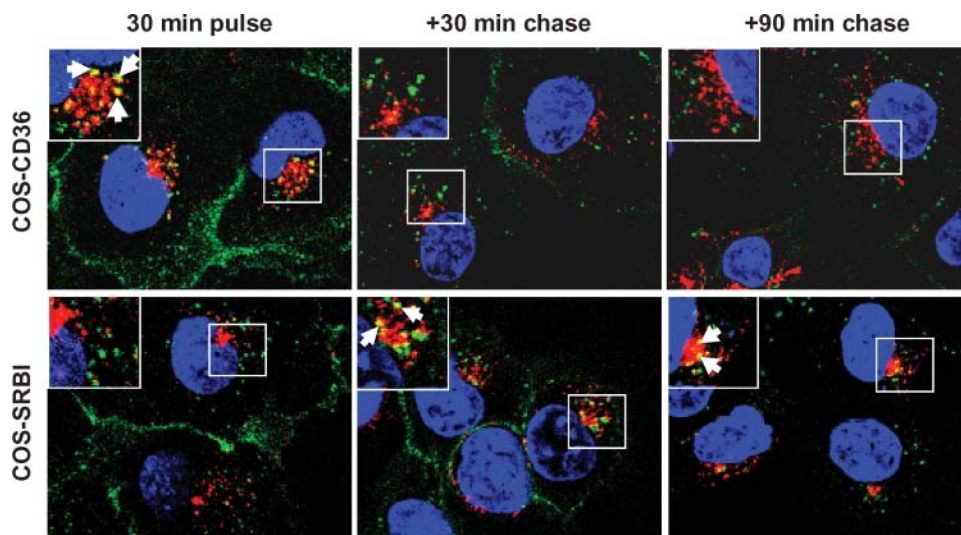


Fig. 2. Intracellular distribution of OxLDL in COS-CD36 and COS-SRBI cells. COS-7 cells expressing CD36 or SR-BI by adenoviral vector were incubated at 37°C with Alexa488-OxLDL (green fluorescence) for 30 min, washed to remove unbound ligand, and then analyzed by confocal microscopy after a 0, 30, or 90 min chase interval. Alexa568-labeled transferrin (red fluorescence) was added during the final 15 min. White boxes indicate regions shown at higher magnification in insets; arrows indicate colocalization of OxLDL and transferrin.

and transferrin was not evident in COS-SRBI cells after the 30 min incubation. Interestingly, the intracellular distribution of OxLDL in COS-SRBI cells after a 30 min chase was similar to that observed in COS-CD36 cells after the shorter time interval (compare COS-CD36, 30 min pulse and COS-SRBI, +30 min chase), at which times the ligand was similarly colocalized with transferrin in the two cell types.

In addition, there appeared to be a marked change in the intracellular distribution of OxLDL in COS-CD36 cells during the 30 min chase, because extensive colocalization with transferrin was no longer evident (compare COS-CD36, 30 min pulse and COS-CD36, +30 min chase). Differences in the intracellular distribution of OxLDL in the two cell types were also apparent after the 90 min chase period (Fig. 2). Whereas colocalization of intracellular OxLDL and transferrin was still evident in COS-SRBI cells, there was little or no evidence of colocalization in COS-CD36 cells at this time point. Thus, results from confocal microscopy provide evidence that the uptake and intracellular trafficking of OxLDL by CD36 and SR-BI is different. Consistent with our quantitative analysis (Fig. 1B), our data indicate that internalization of OxLDL by CD36 may occur at a faster rate compared with SR-BI. Furthermore, OxLDL trafficking into and out of the endocytic recycling compartment in COS-

SRBI cells appears to be delayed compared with that in COS-CD36 cells.

Endocytosis of OxLDL by SR-BI and CD36 is independent of caveolae, microtubules, and actin cytoskeleton

We investigated the role of caveolae in OxLDL uptake by CD36 and SR-BI using nystatin, which disrupts caveolae structure by sequestering cholesterol (33). In a control experiment, nontransfected COS-7 cells were preincubated with 25 $\mu\text{g}/\text{ml}$ nystatin at 37°C for 1 h and then incubated with Alexa488-albumin in the presence of nystatin. Confocal microscopy showed that albumin uptake was blocked by nystatin treatment, as expected (Fig. 3A). However, uptake of Alexa488-OxLDL by COS-CD36 or COS-SRBI cells was not altered by nystatin treatment, as determined by both confocal microscopy (Fig. 3A) and the fluorescence energy transfer assay (Fig. 3B). This result indicates that endocytosis of OxLDL by either class B scavenger receptor is not caveolae-dependent.

The role of cytoskeletal elements in OxLDL uptake was investigated by treating COS-CD36 and COS-SRBI cells with either cytochalasin D or nocodazole, which disrupts actin polymerization or microtubule elongation, respectively. In control experiments, we confirmed that these

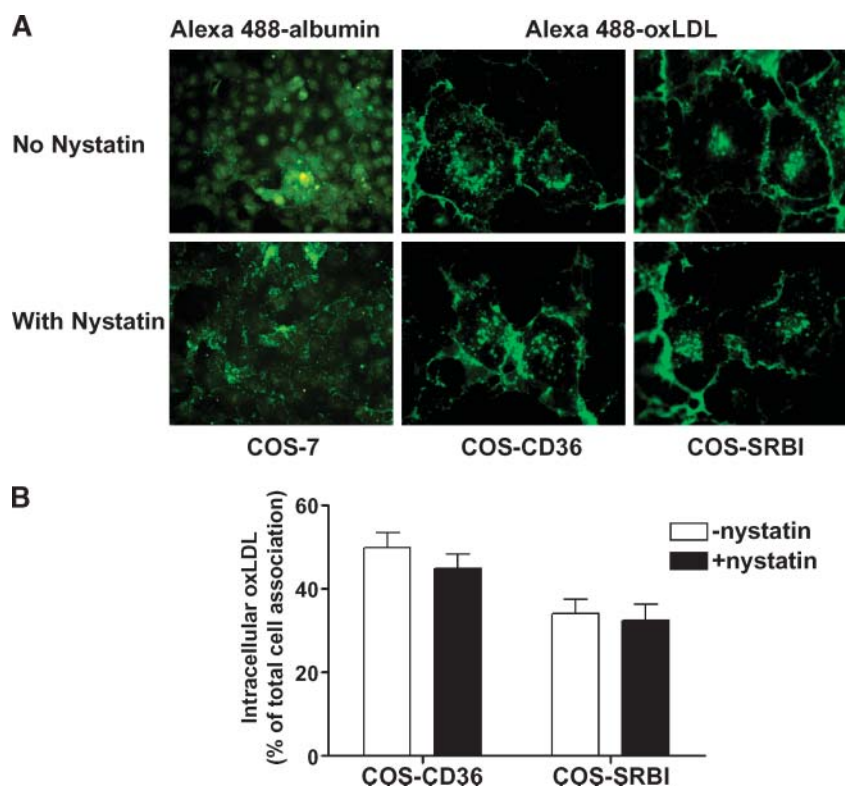


Fig. 3. Lack of a role for caveolae in OxLDL uptake by CD36 and SR-BI. Control COS-7 cells or cells expressing CD36 or SR-BI by adenoviral vector were preincubated in the presence or absence of 25 $\mu\text{g}/\text{ml}$ nystatin at 37°C for 1 h, as indicated. A: Cells were then incubated at 37°C for 30 min with 30 $\mu\text{g}/\text{ml}$ Alexa488-albumin (analyzed by fluorescence microscopy with magnification at 20 \times) or for 1 h with 10 $\mu\text{g}/\text{ml}$ Alexa488-OxLDL (analyzed by confocal microscopy with magnification at 100 \times) with or without 25 $\mu\text{g}/\text{ml}$ nystatin, as indicated. B: Cells were similarly treated and analyzed by fluorescence energy transfer assay. CD36- and SR-BI-specific values are shown and are expressed as the percentage of total cell-associated OxLDL after the 1 h incubation. Values are means \pm SEM of three independent determinations and are representative of two experiments.

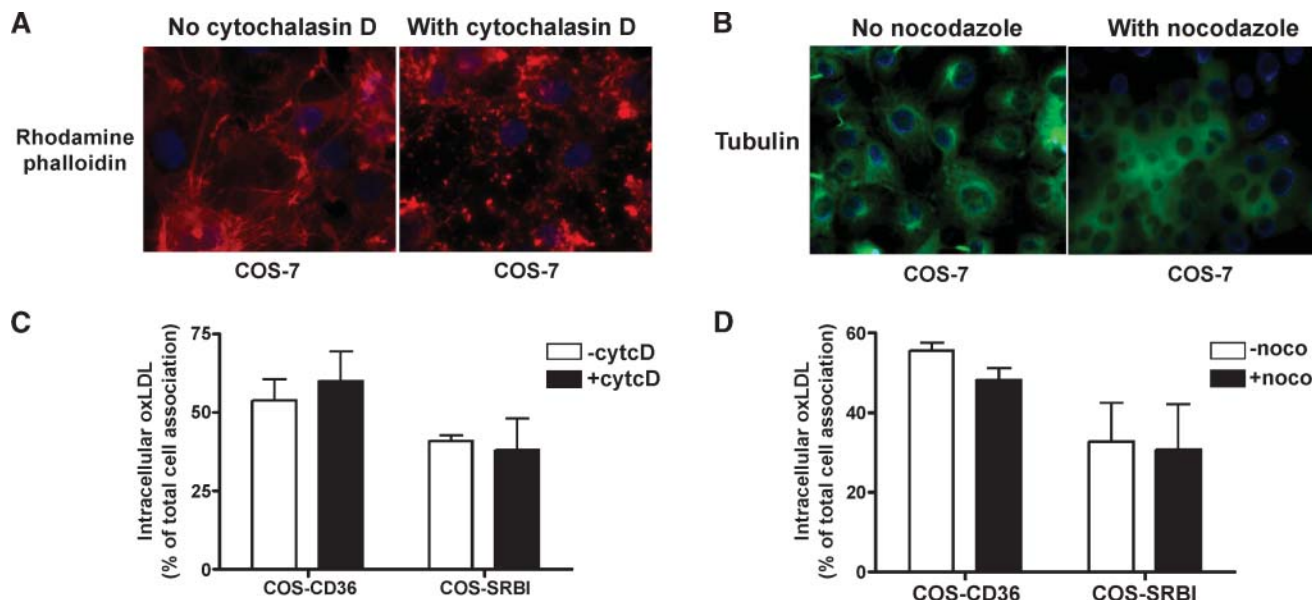


Fig. 4. Lack of a role for actin cytoskeleton or intact microtubules in OxLDL uptake by CD36 and SR-BI. **A:** COS-7 cells with or without preincubation with 10 μ M cytochalasin D were incubated with rhodamine phalloidin and then analyzed by fluorescence microscopy, as described in Experimental Procedures (magnification, 60 \times). **B:** COS-7 cells with or without preincubation with 10 μ M nocodazole were immunostained with Alexa488-conjugated anti-tubulin antibody and then analyzed by fluorescence microscopy, as described in Experimental Procedures (magnification, 60 \times). **C:** Control COS-7, COS-CD36, or COS-SRBI cells were incubated in the presence or absence of 10 μ M cytochalasin D at 37 $^{\circ}$ C for 1 h, as indicated. Intracellular OxLDL was quantified by the fluorescence energy transfer assay. CD36- and SR-BI-specific values are shown and are expressed as the percentage of total cell-associated OxLDL after the 1 h incubation. Values are means \pm SEM of three independent determinations and are representative of two experiments. **D:** Control COS-7, COS-CD36, or COS-SRBI cells were incubated in the presence or absence of 10 μ M nocodazole at 37 $^{\circ}$ C for 1 h, as indicated. Intracellular OxLDL was quantified by the fluorescence energy transfer assay. CD36- and SR-BI-specific values are shown and are expressed as the percentage of total cell-associated OxLDL after the 1 h incubation. Values are means \pm SEM of triplicate determinations and are representative of two independent experiments.

reagents had the expected effect on cell morphology of nontransfected COS-7 cells (Fig. 4A, B) (34, 35). However, there was no evidence that these agents interfered with OxLDL uptake by either COS-CD36 or COS-SRBI cells, as determined by confocal microscopy (data not shown) or the fluorescence energy transfer assay (Fig. 4C, D). Thus, OxLDL uptake by CD36 or SR-BI does not depend on an intact actin cytoskeleton or microtubules.

Endocytosis of OxLDL by CD36, but not SR-BI, is dynamin-dependent

The GTPase dynamin plays a role in the fission of endocytic vesicles from the plasma membrane (36). To study the role of dynamin in OxLDL endocytosis by class B scavenger receptors, a dominant-negative mutant of dynamin-1 (dynK44A) was expressed in COS-CD36 and COS-SRBI cells and the effect on OxLDL degradation was determined. In a control experiment, we determined the effect of dynK44A expression on the uptake of 125 I-transferrin, which is known to be endocytosed via a dynamin-dependent pathway. Interestingly, expression of dynK44A significantly reduced OxLDL degradation by COS-CD36 cells but not COS-SRBI cells (Fig. 5A). The partial inhibition (\sim 40%) of CD36-mediated OxLDL degradation by dynK44A likely reflects the extent to which the dominant-negative mutant blocks dynamin function in our studies,

because cells expressing dynK44A showed only a 50% decrease in 125 I-transferrin uptake (Fig. 5B).

The dynamin dependence of OxLDL uptake was also assessed using fluorescently labeled OxLDL and confocal microscopy (Fig. 5C). For these experiments, COS-CD36 and COS-SRBI cells with and without dynK44A expression were incubated with Alexa488-OxLDL (green fluorescence) for 1 h. To monitor the extent to which dynamin function was inhibited by dynK44A in individual cells, Alexa568-transferrin (red fluorescence) was added during the final 15 min of incubation. Uptake of both OxLDL and transferrin could easily be detected in control COS-CD36 and COS-SRBI cells (Fig. 5C, upper panels). The amount of internalized transferrin was variable in COS-CD36 and COS-SRBI cells expressing dynK44A, indicating that dynamin-dependent endocytosis was not completely blocked in all cells (data not shown). However, an absence of intracellular transferrin was clearly observed in a subset of the treated cells, indicating effective inhibition of dynamin activity (Fig. 5C). For COS-CD36 cells exhibiting a total block in transferrin uptake, virtually all of the OxLDL appeared to be at or near the cell surface (Fig. 5C, lower left panel). In contrast, there was no apparent difference in the uptake of OxLDL in control COS-SRBI cells and cells in which dynamin-dependent uptake of transferrin was effectively inhibited (Fig. 5C, right panels).

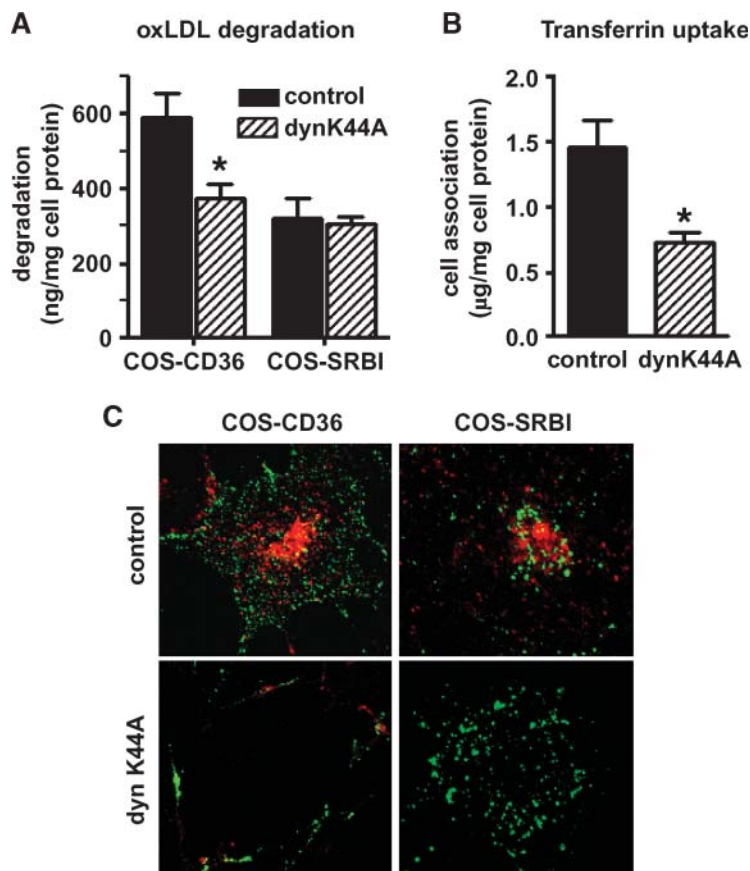


Fig. 5. Dynamine dependence of OxLDL uptake by CD36. CD36, SR-BI, and dynK44A (a dominant-negative mutant of dynamin 1) were expressed in COS-7 cells by adenoviral vector, as indicated. A: Cells were incubated with 10 $\mu\text{g/ml}$ ^{125}I -OxLDL at 37°C for 4 h, and OxLDL apolipoprotein degradation was quantified. B: COS-7 cells were incubated with 25 $\mu\text{g/ml}$ ^{125}I -transferrin for 15 min. Values shown are means \pm SEM (* $P < 0.05$) of three determinations and are representative of three independent experiments. C: Cells were incubated with 10 $\mu\text{g/ml}$ Alexa488-OxLDL at 37°C for 45 min followed by 15 min of coin-cubation with 20 $\mu\text{g/ml}$ Alexa568-transferrin. Cells were washed and then analyzed by confocal microscopy.

We next investigated the possibility that dynamin plays a role in CD36-mediated uptake of OxLDL in macrophages. Peritoneal macrophages from wild-type C57BL/6 mice and C57BL/6 mice deficient in CD36 (CD36^{-/-}) were incubated for 1 h with Alexa568-OxLDL (red fluorescence) and then visualized by confocal microscopy. As expected, CD36^{-/-} macrophages appeared to accumulate less intracellular OxLDL compared with C57BL/6 macrophages (Fig. 6). OxLDL taken up by C57BL/6 cells showed extensive colocalization with dynamin (green fluorescence) that was evident both intracellularly and at or near the cell surface (Fig. 6, inset A). Substantially less colocalization of OxLDL and dynamin was apparent in CD36^{-/-} cells (Fig. 6, inset B).

The CD36 C-terminal cytoplasmic domain confers dynamine dependence of OxLDL uptake

The C-terminal six amino acids of CD36 have been shown to be critical for endocytosis and degradation of OxLDL (15). To investigate the role of the CD36 cytoplasmic "tail" in dynamine-dependent uptake, we studied OxLDL uptake by CD36/SR-BI chimeric receptors, in which the amino acid sequences corresponding to the intracellular

C-terminal domain of the respective receptors were interchanged (23, 24). COS cells expressing wild-type rat CD36, mouse SR-BI, CD/SRT (CD36 residues 1–458 and SR-BI residues 464–509) or SR/CDT (SR-BI residues 1–467 and CD36 residues 459–472) were analyzed by immunoblotting to confirm receptor expression (Fig. 7A). As expected, antisera raised against full-length mouse CD36 (26) recognized wild-type CD36, CD/SRT, and to a lesser extent SR/CDT, whereas anti-BI⁴⁹⁵ [an anti-peptide antibody raised against SR-BI residues 495–509 (25)] interacted only with wild-type SR-BI and CD/SRT (Fig. 7A). Control COS cells expressing either CD/SRT or SR/CDT readily took up Alexa488-OxLDL (Fig. 7B). However, expression of dynK44A blocked OxLDL uptake by SR/CDT but not CD/SRT. This result demonstrates that the C-terminal cytoplasmic tail of CD36 is necessary and sufficient for dynamine-dependent OxLDL uptake by class B scavenger receptors.

DISCUSSION

CD36 and SR-BI are class B scavenger receptors that share significant structural and sequence homology and bind with

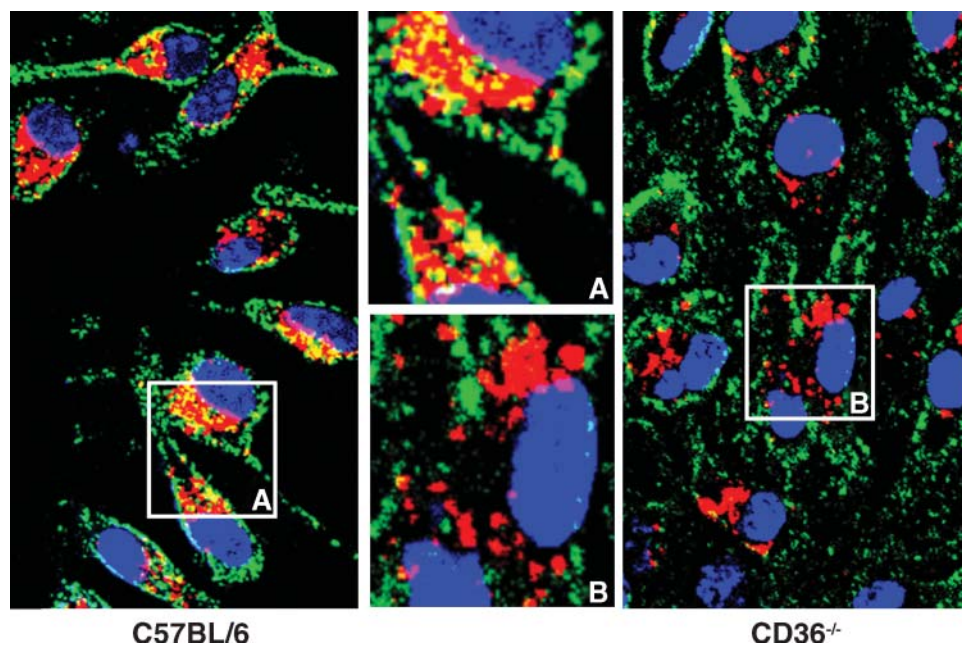


Fig. 6. The colocalization of intracellular OxLDL and dynamin in macrophages is CD36-dependent. Peritoneal macrophages isolated from wild-type mice (left panel) and mice deficient in CD36 (right panel) were incubated with Alexa568-OxLDL (red fluorescence) for 1 h at 37°C. Cells were immunostained to detect dynamin (green fluorescence) and then analyzed by confocal microscopy. White boxes indicate regions shown at higher magnification in the middle panels.

high affinity a wide variety of lipoprotein ligands, including HDL and OxLDL. Despite these similarities, CD36 and SR-BI are considered to have very distinct functions in lipoprotein metabolism. The importance of CD36 in macrophage foam cell formation has been well documented *in vitro* by its substantial capacity to endocytose and degrade OxLDL (1, 2). On the other hand, the major function of SR-BI is to mediate the transfer of cholesteryl ester from HDL to cells by a selective lipid uptake process in which HDL proteins are not intracellularly degraded. In addition, SR-BI has been shown to facilitate the efflux of excess cellular cholesterol to HDL. To date, the molecular pathways that underlie differences in OxLDL and HDL metabolism by CD36 and SR-BI are not well understood. In this study, we directly compared the uptake, intracellular trafficking, and degradation of OxLDL by CD36 and SR-BI. The major findings of these studies are as follows: 1) relative to total cell-associated OxLDL, CD36 mediates more efficient OxLDL degradation than SR-BI; 2) OxLDL uptake by SR-BI and CD36 is independent of caveolae, microtubules, and actin cytoskeleton; 3) endocytosis of OxLDL by CD36, but not SR-BI, is dynamin-dependent; and 4) the cytoplasmic C-terminal tail of CD36 confers dynamin dependence of OxLDL uptake.

Our results show that after 4 h of incubation at 37°C, COS-7 cells expressing CD36 mediate ~2-fold more OxLDL degradation than SR-BI-expressing cells when normalized to OxLDL cell association. We investigated whether differences in the amount of OxLDL taken up by the two receptors could explain this discrepancy. We determined that the fraction of the total cell-associated

OxLDL that had accumulated intracellularly in CD36-expressing cells was consistently larger compared with that of SR-BI-expressing cells, although the difference was not statistically significant. It should be noted that the difference in OxLDL internalization between the two cell types may be underestimated in our experiments, because the fluorescence-based assay would not take into account the greater amount of OxLDL degradation that occurs in COS-CD36 cells compared with COS-SRBI cells.

Although studies *in vitro* demonstrate a significant role for CD36 in the uptake and degradation of OxLDL by human (37) and mouse (12) macrophages, insights into the molecular details of CD36-mediated endocytosis and subsequent intracellular trafficking of OxLDL are limited. An initial study in lung tissue localized CD36 to lipid rafts/caveolae (33). However, a more recent study indicated that CD36 expressed in CHO cells is localized to lipid rafts but not caveolae, and the binding of OxLDL to CD36 leads to endocytosis through a lipid raft pathway that is distinct from clathrin- or caveolin-mediated internalization pathways (14). Our results in COS-7 cells support the conclusion that CD36 internalizes OxLDL by a clathrin- and caveolin-independent pathway. Although SR-BI has been reported to be localized to caveolae in several cell lines, SR-BI-mediated HDL-selective cholesteryl ester uptake does not appear to be caveolin-dependent (27). Here, we show that nystatin, which disrupts caveolae structure by sequestering cholesterol, has no effect on the intracellular accumulation of OxLDL mediated by SR-BI. Our data also show that treatment with nocodazole or cytochalasin D does not reduce OxLDL uptake by either

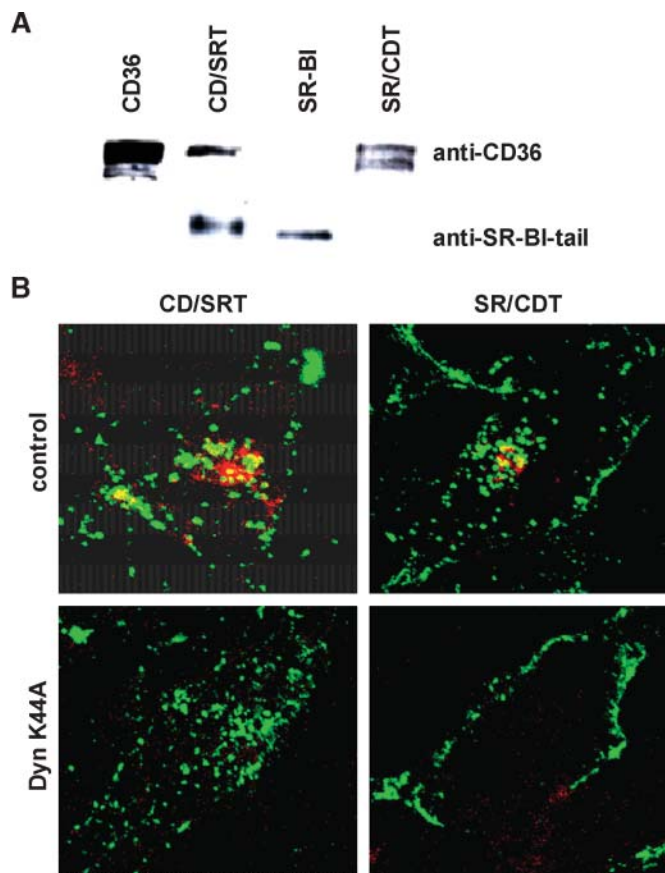


Fig. 7. Dynamin dependence of OxLDL uptake by chimeric CD36/SR-BI receptors. Wild-type rat CD36, mouse SR-BI, and chimeric CD/SRT or SR/CDT receptors were expressed in COS cells as described in Experimental Procedures. A: Immunoblot analysis of total cell lysates (20 μ g of protein) was performed using anti-mouse CD36 (top panel) or anti-BI⁴⁹⁵, which recognizes the C-terminal cytoplasmic domain of SR-BI (bottom panel). B: COS cells expressing CD/SRT or SR/CDT with and without adenovirus expression of dynK44A, as indicated, were incubated with 10 μ g/ml Alexa488-OxLDL at 37°C for 45 min followed by 15 min of coincubation with 20 μ g/ml Alexa568-transferrin. Cells were washed and then analyzed by confocal microscopy.

CD36 or SR-BI, indicating that microtubules and actin cytoskeleton are not involved in the endocytosis of OxLDL by either receptor. However, we cannot rule out the possibility that these elements play a role in the subsequent intracellular trafficking of OxLDL.

Receptor-mediated endocytosis involves the formation of endocytic vesicles followed by membrane fission. The molecular mechanisms driving fission have been studied extensively, and it is now clear that many fission events are controlled by three closely related (>80% identical) isoforms of dynamin. Dynamin, a \sim 100 kDa GTPase, has been implicated in both clathrin-mediated and caveolae-mediated endocytosis as well as in clathrin- and caveolae-independent endocytic events (38–40). Our data clearly show that OxLDL degradation in COS-CD36 cells is reduced significantly in cells expressing a dominant-negative mutant of dynamin (dynK44A). We also show that in mouse peritoneal macrophages, dynamin colo-

calizes with intracellular OxLDL in a CD36-dependent manner. Together, our data strongly suggest that dynamin plays an important role in CD36-mediated OxLDL endocytosis in macrophages.


A role for dynamin in OxLDL uptake has also been demonstrated in vascular smooth muscle cells (VSMCs) (41). In this study, dynamin-2 was shown to colocalize with OxLDL in the cytoplasm of VSMCs, leading the authors to conclude that dynamin is involved in scavenger receptor-mediated OxLDL endocytosis in these cells. Expression of dynK44A significantly reduced OxLDL endocytosis, as well as OxLDL-induced apoptosis, in VSMCs. Interestingly, the addition of OxLDL to VSMCs resulted in the movement of dynamin-2 from the cytoplasm to the cell surface, where it colocalized with lectin-like oxidized low density lipoprotein receptor 1. The authors reported that dynamin-2 also colocalized with CD36; however, the data for this statement were not presented. Our data from the analysis of macrophages differ from the previous report involving VSMCs in that we failed to find a global movement of dynamin to the cell surface induced by OxLDL (data not shown). Although we did not specifically address the role of lectin-like oxidized low density lipoprotein receptor 1 in our studies, the observation that the colocalization of intracellular OxLDL and dynamin is reduced significantly in mouse peritoneal macrophages lacking CD36 suggests that other scavenger receptors play only a minor role in dynamin-dependent OxLDL uptake in these cells.

It is increasingly apparent that not all endocytic events are dependent on dynamin, suggesting the existence of other fission machineries. For example, G-protein AT1A angiotensin receptors and M2 muscarinic receptors are internalized by a dynamin-independent pathway (42, 43). Bonazzi et al. (44) recently reported that CtBP3/BARS controls the formation of transport vesicles that are operative in endocytic and exocytic pathways that do not require dynamin. Here, we show that, unlike CD36, SR-BI mediates OxLDL uptake through a pathway that is independent of dynamin. Endocytosis of HDL by SR-BI has also been shown to be dynamin-independent (27). By analyzing chimeric CD36/SR-BI receptors, we determined that the 14 amino acid C-terminal domain of CD36 (constituting the C-terminal cytoplasmic tail) is necessary and sufficient to confer dynamin-dependent OxLDL endocytosis. This domain has also been shown to be required for the binding, internalization, and degradation of OxLDL by CD36 (26).

Our analysis by confocal microscopy suggests that the trafficking into and out of the endocytic recycling compartment may be slower for OxLDL internalized by SR-BI compared with CD36. This conclusion is consistent with previous evidence that different endocytic mechanisms may participate in vesicular trafficking to distinct intracellular locations. In an elegant study, Vickery and von Zastrow (45) investigated the endocytic membrane trafficking of D1 and D2 dopamine receptors, two structurally homologous G protein-coupled receptors. These receptors were shown to selectively endocytose in the same cells by distinct dynamin-dependent and -independent mechanisms. Interestingly, these endocytic pathways differed in their physiological

regulation, and they delivered D1 and D2 to different primary endocytic vesicles. Although the mechanism of dynamin-independent endocytosis of D2 receptors was not elucidated, it was noted that the cytoplasmic domains of D1 and D2 are not well conserved. These findings demonstrate that molecular sorting of structurally homologous receptors can occur at the plasma membrane.

Our studies provide the new finding that OxLDL taken up by the structurally related class B scavenger receptors SR-BI and CD36 may be selectively sorted at the plasma membrane into different endocytic pathways. Although it was not possible in our studies to determine the extent to which OxLDL taken up by these two pathways remains segregated or converges, it is notable that pulse-chase studies revealed differences in the apparent intracellular trafficking of OxLDL in COS-CD36 and COS-SRBI cells. Whereas little OxLDL could be detected after 30 min in COS-SRBI cells, OxLDL in COS-CD36 cells was easily observed in a perinuclear compartment, colocalized with transferrin. After 60 min (30 min pulse followed by 30 min chase), OxLDL was widely distributed in a punctate pattern throughout COS-CD36 cells, separate from transferrin. At this time point, intracellular OxLDL could be visualized in the perinuclear region of COS-SRBI cells, colocalized with transferrin. Thus, OxLDL initially trafficks through a transferrin-positive compartment in both CD36- and SR-BI-expressing cells, but transit to this compartment in SR-BI-expressing cells appears to be slower compared with that in CD36. This suggests that OxLDL may be differentially distributed among distinct endocytic vesicles in the two cell types. Based on these observations, it is possible that OxLDL transits through analogous intracellular compartments but with different kinetics after uptake by CD36 or SR-BI. However, given the difference in the efficiency of OxLDL degradation by the two class B scavenger receptors, it is likely that uptake by CD36 and SR-BI destines OxLDL to differential intracellular trafficking through distinct pathways.

In summary, we have shown that uptake of OxLDL by CD36 and SR-BI occurs through distinct endocytic mechanisms dictated by their respective C-terminal cytoplasmic tails. This finding identifies a novel functional property that distinguishes these structurally homologous receptors, which may have important implications with regard to lipoprotein metabolism by these two receptors. 

This work was funded by an American Heart Association Predoctoral Training Grant (to B.S.), an American Heart Association Scientific Development Grant (to N.R.W.), and National Institutes of Health Grant HL-63763 (to D.R.v.d.W.).

REFERENCES

- Endemann, G., L. W. Stanton, K. S. Madden, C. M. Bryant, R. T. White, and A. A. Protter. 1993. CD36 is a receptor for oxidized low density lipoprotein. *J. Biol. Chem.* **268**: 11811–11816.
- Moore, K. J., and M. W. Freeman. 2006. Scavenger receptors in atherosclerosis: beyond lipid uptake. *Arterioscler. Thromb. Vasc. Biol.* **26**: 1702–1711.
- Asch, A. S., J. Barnwell, R. L. Silverstein, and R. L. Nachman. 1987. Isolation of the thrombospondin membrane receptor. *J. Clin. Invest.* **79**: 1054–1061.
- Calvo, D., D. Gomez-Coronado, Y. Suarez, M. A. Lasuncion, and M. A. Vega. 1998. Human CD36 is a high affinity receptor for the native lipoproteins HDL, LDL, and VLDL. *J. Lipid Res.* **39**: 777–788.
- Abumrad, N., C. Harmon, and A. Ibrahim. 1998. Membrane transport of long-chain fatty acids: evidence for a facilitated process. *J. Lipid Res.* **39**: 2309–2318.
- Rigotti, A., S. L. Acton, and M. Krieger. 1995. The class B scavenger receptors SR-BI and CD36 are receptors for anionic phospholipids. *J. Biol. Chem.* **270**: 16221–16224.
- Ren, Y., R. L. Silverstein, J. Allen, and J. Savill. 1995. CD36 gene transfer confers capacity for phagocytosis of cells undergoing apoptosis. *J. Exp. Med.* **181**: 1857–1862.
- Febbraio, M., D. P. Hajjar, and R. L. Silverstein. 2001. CD36: a class B scavenger receptor involved in angiogenesis, atherosclerosis, inflammation, and lipid metabolism. *J. Clin. Invest.* **108**: 785–791.
- Murphy, J. E., P. R. Tedbury, S. Homer-Vanniasinkam, J. H. Walker, and S. Ponnambalam. 2005. Biochemistry and cell biology of mammalian scavenger receptors. *Atherosclerosis*. **182**: 1–15.
- Kunjathoor, V. V., M. Febbraio, E. A. Podrez, K. J. Moore, L. Andersson, S. Koehn, J. S. Rhee, R. Silverstein, H. F. Hoff, and M. W. Freeman. 2002. Scavenger receptors class A-I/II and CD36 are the principal receptors responsible for the uptake of modified low density lipoprotein leading to lipid loading in macrophages. *J. Biol. Chem.* **277**: 49982–49988.
- Podrez, E. A., M. Febbraio, N. Sheibani, D. Schmitt, R. L. Silverstein, D. P. Hajjar, P. A. Cohen, W. A. Frazier, H. F. Hoff, and S. L. Hazen. 2000. Macrophage scavenger receptor CD36 is the major receptor for LDL modified by monocyte-generated reactive nitrogen species. *J. Clin. Invest.* **105**: 1095–1108.
- Febbraio, M., E. A. Podrez, J. D. Smith, D. P. Hajjar, S. L. Hazen, H. F. Hoff, K. Sharma, and R. L. Silverstein. 2000. Targeted disruption of the class B scavenger receptor CD36 protects against atherosclerotic lesion development in mice. *J. Clin. Invest.* **105**: 1049–1056.
- Zhao, S. P., J. Wu, D. Q. Zhang, H. J. Ye, L. Liu, and J. Q. Li. 2004. Fenofibrate enhances CD36 mediated endocytic uptake and degradation of oxidized low density lipoprotein in adipocytes from hypercholesterolemia rabbit. *Atherosclerosis*. **177**: 255–262.
- Zeng, Y., N. Tao, K. N. Chung, J. E. Heuser, and D. M. Lublin. 2003. Endocytosis of oxidized low density lipoprotein through scavenger receptor CD36 utilizes a lipid raft pathway that does not require caveolin-1. *J. Biol. Chem.* **278**: 45931–45936.
- Malaud, E., D. Hourton, L. M. Giroux, E. Ninio, R. Buckland, and J. L. McGregor. 2002. The terminal six amino-acids of the carboxy cytoplasmic tail of CD36 contain a functional domain implicated in the binding and capture of oxidized low-density lipoprotein. *Biochem. J.* **364**: 507–515.
- Acton, S. L., P. E. Scherer, H. F. Lodish, and M. Krieger. 1994. Expression cloning of SR-BI, a CD36-related class B scavenger receptor. *J. Biol. Chem.* **269**: 21003–21009.
- Calvo, D., D. Gomez-Coronado, M. A. Lasuncion, and M. A. Vega. 1997. CLA-1 is an 85-kD plasma membrane glycoprotein that acts as a high-affinity receptor for both native (HDL, LDL, and VLDL) and modified (OxLDL and AcLDL) lipoproteins. *Arterioscler. Thromb. Vasc. Biol.* **17**: 2341–2349.
- Gillotte-Taylor, K., A. Boullier, J. L. Witztum, D. Steinberg, and O. Quehenberger. 2001. Scavenger receptor class B type I as a receptor for oxidized low density lipoprotein. *J. Lipid Res.* **42**: 1474–1482.
- Hirano, K., S. Yamashita, Y. Nakagawa, T. Ohya, F. Matsuura, K. Tsukamoto, Y. Okamoto, A. Matsuyama, K. Matsumoto, J. Miyagawa, et al. 1999. Expression of human scavenger receptor class B type I in cultured human monocyte-derived macrophages and atherosclerotic lesions. *Circ. Res.* **85**: 108–116.
- Buechler, C., M. Ritter, C. D. Quoc, A. Agildere, and G. Schmitz. 1999. Lipopolysaccharide inhibits the expression of the scavenger receptor Cla-I in human monocytes and macrophages. *Biochem. Biophys. Res. Commun.* **262**: 251–254.
- Chinetti, G., F. G. Gbaguidi, S. Griglio, Z. Mallat, M. Antonucci, P. Poulain, J. Chapman, J. C. Fruchart, A. Tedgui, J. Najib-Fruchart, et al. 2000. CLA-1/SR-BI is expressed in atherosclerotic lesion macrophages and regulated by activators of peroxisome proliferator-activated receptors. *Circulation*. **101**: 2411–2417.
- Febbraio, M., N. A. Abumrad, D. P. Hajjar, K. Sharma, W. Cheng, S. F. A. Pearce, and R. L. Silverstein. 1999. A null mutation in

- murine CD36 reveals an important role in fatty acid and lipoprotein metabolism. *J. Biol. Chem.* **274**: 19055–19062.
23. Connelly, M. A., S. M. Klein, S. Azhar, N. A. Abumrad, and D. L. Williams. 1999. Comparison of class B scavenger receptors, CD36 and scavenger receptor BI (SR-BI), shows that both receptors mediate high density lipoprotein-cholesteryl ester selective uptake but SR-BI exhibits a unique enhancement of cholesteryl ester uptake. *J. Biol. Chem.* **274**: 41–47.
 24. Connelly, M. A., M. de la Llera-Moya, P. Monzo, P. G. Yancey, D. Drazul, G. Stoudt, N. Fournier, S. M. Klein, G. H. Rothblat, and D. L. Williams. 2001. Analysis of chimeric receptors shows that multiple distinct functional activities of scavenger receptor, class B, type I (SR-BI), are localized to the extracellular receptor domain. *Biochemistry*. **40**: 5249–5259.
 25. Webb, N. R., P. M. Connell, G. A. Graf, E. J. Smart, W. J. S. de Villiers, F. C. de Beer, and D. R. van der Westhuyzen. 1998. SR-BII, an isoform of the scavenger receptor BI containing an alternate cytoplasmic tail, mediates lipid transfer between high density lipoprotein and cells. *J. Biol. Chem.* **273**: 15241–15248.
 26. de Villiers, W. J. S., L. Cai, N. R. Webb, M. C. de Beer, D. R. van der Westhuyzen, and F. C. de Beer. 2001. CD36 does not play a direct role in HDL or LDL metabolism. *J. Lipid Res.* **42**: 1231–1238.
 27. Silver, D. L., N. Wang, X. Xiao, and A. R. Tall. 2001. High density lipoprotein (HDL) particle uptake mediated by scavenger receptor class B type I results in selective sorting of HDL cholesterol from protein and polarized cholesterol secretion. *J. Biol. Chem.* **276**: 25287–25293.
 28. Strachan, A. F., F. C. de Beer, D. R. van der Westhuyzen, and G. A. Coetzee. 1988. Identification of three isoform patterns of human serum amyloid A protein. *Biochem. J.* **250**: 203–207.
 29. Lowry, O. H., N. J. Rosebrough, A. L. Farr, and B. J. Randall. 1951. Protein measurement with the Folin phenol reagent. *J. Biol. Chem.* **193**: 265–275.
 30. Bilheimer, D. W., S. Eisenberg, and R. I. Levy. 1972. The metabolism of very low density lipoproteins. *Biochim. Biophys. Acta.* **260**: 212–221.
 31. Bierman, E. L., O. Stein, and Y. Stein. 1974. Lipoprotein uptake and metabolism by rat aortic smooth muscle cells in tissue culture. *Circ. Res.* **35**: 136–150.
 32. Sun, B., E. R. Eckhardt, S. Shetty, D. R. van der Westhuyzen, and N. R. Webb. 2006. Quantitative analysis of SR-BI-dependent HDL retroendocytosis in hepatocytes and fibroblasts. *J. Lipid Res.* **47**: 1700–1713.
 33. Lisanti, M. P., P. E. Schere, J. Vidugiriene, Z. Tang, A. Hermanowski-Vosatka, Y. H. Tu, R. F. Cook, and M. Sargiacomo. 1994. Characterization of caveolin-rich membrane domains isolated from an endothelial-rich source: implications for human disease. *J. Cell Biol.* **126**: 111–126.
 34. Samson, F., J. A. Donoso, I. Heller-Bettinger, D. Watson, and R. H. Himes. 1979. Nocodazole action on tubulin assembly, axonal ultrastructure and fast axoplasmic transport. *J. Pharmacol. Exp. Ther.* **208**: 411–417.
 35. Cooper, J. A. 1987. Effects of cytochalasin and phalloidin on actin. *J. Cell Biol.* **105**: 1473–1478.
 36. Sever, S. 2002. Dynamin and endocytosis. *Curr. Opin. Cell Biol.* **14**: 463–467.
 37. Nozaki, S., H. Kashiwagi, S. Yamashita, T. Nakagawa, B. Kostner, Y. Tomiyama, A. Nakata, M. Ishigami, J. Miyagawa, K. Kameda-Takemura, et al. 1995. Reduced uptake of oxidized low density lipoproteins in monocyte-derived macrophages from CD36-deficient subjects. *J. Clin. Invest.* **96**: 1859–1865.
 38. Oh, P., D. P. McIntosh, and J. E. Schnitzer. 1998. Dynamin at the neck of caveolae mediates their budding to form transport vesicles by GTP-driven fission from the plasma membrane of endothelium. *J. Cell Biol.* **141**: 101–114.
 39. Pelkmans, L., and A. Helenius. 2002. Endocytosis via caveolae. *Traffic*. **3**: 311–320.
 40. Nichols, B. J., and J. Lippincott-Schwartz. 2001. Endocytosis without clathrin coats. *Trends Cell Biol.* **11**: 406–412.
 41. Kashiwakura, Y., M. Watanabe, N. Kusumi, K. Sumiyoshi, Y. Nasu, H. Yamada, T. Sawamura, H. Kumon, K. Takei, and H. Daida. 2004. Dynamin-2 regulates oxidized low-density lipoprotein-induced apoptosis of vascular smooth muscle cell. *Circulation*. **110**: 3329–3334.
 42. Zhang, J., S. S. Ferguson, L. S. Barak, L. Menard, and M. G. Caron. 1996. Dynamin and beta-arrestin reveal distinct mechanisms for G protein-coupled receptor internalization. *J. Biol. Chem.* **271**: 18302–18305.
 43. Pals-Rylaarsdam, R., V. V. Gurevich, K. B. Lee, J. A. Ptasinski, J. L. Benovic, and M. M. Hosey. 1997. Internalization of the m2 muscarinic acetylcholine receptor. Arrestin-independent and -dependent pathways. *J. Biol. Chem.* **272**: 23682–23689.
 44. Bonazzi, M., S. Spano, G. Turacchio, C. Cericola, C. Valente, A. Colanzi, H. S. Kweon, V. W. Hsu, E. V. Polishchuck, R. S. Polishchuck, et al. 2005. CtBP3/BARS drives membrane fission in dynamin-independent transport pathways. *Nat. Cell Biol.* **7**: 570–580.
 45. Vickery, R. G., and M. von Zastrow. 1999. Distinct dynamin-dependent and -independent mechanisms target structurally homologous dopamine receptors to different endocytic membranes. *J. Cell Biol.* **144**: 31–43.